

# Ultra-stability Yb-doped fiber optical frequency comb with $2 \times 10^{-18}/\text{s}$ stability in-loop

LIHUI PANG,<sup>1</sup> HAINIAN HAN,<sup>1</sup> ZHIBIN ZHAO,<sup>2</sup> WENJUN LIU,<sup>1,3</sup> AND ZHIYI WEI<sup>1,\*</sup>

<sup>1</sup>Beijing National Laboratory for Condensed Matter Physics, Institute of Physics, Chinese Academy of Sciences, Beijing 100190, China

<sup>2</sup>Beijing Ruidaen Technology Co., LTD, Beijing 100094, China

<sup>3</sup>State Key Laboratory of Information Photonics and Optical Communications, School of Science, Beijing University of Posts and Telecommunications, Beijing 100876, China

\*zywei@iphy.ac.cn

**Abstract:** We demonstrate a full control ultra-stability Yb-doped fiber optical frequency comb (OFC). The carrier-envelope offset frequency ( $f_{\text{ceo}}$ ) and the repetition rate ( $f_r$ ) are locked with the standard phase locked loop (PLL) technique. The  $f_{\text{ceo}}$  is locked to the radio frequency (RF) synthesizer, and the Allan deviation is  $1.2 \times 10^{-17}/\text{s}$ . The  $f_r$  is locked to an ultra-stability continuous wave (CW) laser at 972 nm. The beat signal ( $f_{\text{beat}}$ ) between the Yb-doped fiber OFC and CW laser is obtained with the signal to noise ratio (SNR) of 43 dB at 300 kHz resolution bandwidth (RBW). The time jitter of the  $f_{\text{beat}}$  signal is 278 as, which is integrated from 1 Hz to 10 MHz. The long-term stability is 575  $\mu\text{Hz}$  in 3 hours, and the corresponding Allan deviation is  $2 \times 10^{-18}/\text{s}$ , which is the best stability result in Yb-doped fiber OFC. The linewidth is narrowed from 200 kHz to subhertz magnitude limited by the instrument resolution bandwidth.

© 2016 Optical Society of America

**OCIS codes:** (120.3930) Metrological instrumentation; (140.3425) Laser stabilization; (120.4800) Optical standards and testing; (140.4050) Mode-locked lasers; (120.3940) Metrology.

## References and links

1. T. W. Hänsch, "Nobel lecture: passion for precision," *Rev. Mod. Phys.* **78**(4), 1297–1309 (2006).
2. J. L. Hall, "Nobel Lecture: Defining and measuring optical frequencies," *Rev. Mod. Phys.* **78**(4), 1279–1295 (2006).
3. J. Ye, H. Schnatz, and L. W. Hollberg, "Optical frequency combs: from frequency metrology to optical phase control," *IEEE J. Sel. Top. Quantum Electron.* **9**(4), 1041–1058 (2003).
4. S. T. Cundiff and J. Ye, "Colloquium: Femtosecond optical frequency combs," *Rev. Mod. Phys.* **75**(1), 325–342 (2003).
5. N. R. Newbury, "Searching for applications with a fine-tooth comb," *Nat. Photonics* **5**(4), 186–188 (2011).
6. T. Steinmetz, T. Wilken, C. Araujo-Hauck, R. Holzwarth, T. W. Hänsch, L. Pasquini, A. Manescau, S. D'Odorico, M. T. Murphy, T. Kentscher, W. Schmidt, and T. Udem, "Laser frequency combs for astronomical observations," *Science* **321**(5894), 1335–1337 (2008).
7. S. A. Diddams, T. Udem, J. C. Bergquist, E. A. Curtis, R. E. Drullinger, L. Hollberg, W. M. Itano, W. D. Lee, C. W. Oates, K. R. Vogel, and D. J. Wineland, "An optical clock based on a single trapped  $^{199}\text{Hg}^+$  ion," *Science* **293**(5531), 825–828 (2001).
8. J. Kim, J. A. Cox, J. Chen, and F. X. Kärtner, "Drift-free femtosecond timing synchronization of remote optical and microwave sources," *Nat. Photonics* **2**(12), 733–736 (2008).
9. T. M. Fortier, M. S. Kirchner, F. Quinlan, J. Taylor, J. C. Bergquist, T. Rosenband, N. Lemke, A. Ludlow, Y. Jiang, C. W. Oates, and S. A. Diddams, "Generation of ultrastable microwave via optical frequency division," *Nat. Photonics* **5**(7), 425–429 (2011).
10. J. Millo, R. Boudot, M. Lours, P. Y. Bourgeois, A. N. Luiten, Y. Le Coq, Y. Kersalé, and G. Santarelli, "Ultra-low-noise microwave extraction from fiber-based optical frequency comb," *Opt. Lett.* **34**(23), 3707–3709 (2009).
11. T. Yasui, S. Yokoyama, H. Inaba, K. Minoshima, T. Nagatsuma, and T. Araki, "Terahertz frequency metrology based on frequency comb," *IEEE J. Sel. Top. Quantum Electron.* **17**(1), 191–201 (2011).
12. A. Ruehl, A. Marcinkiewicz, M. E. Fermann, and I. Hartl, "80 W, 120 fs Yb-fiber frequency comb," *Opt. Lett.* **35**(18), 3015–3017 (2010).

13. T. C. Schratwieser, K. Balskus, R. A. McCracken, C. Farrell, C. G. Leburn, Z. Zhang, T. P. Lamour, T. I. Ferreira, A. Marandi, A. S. Arnold, and D. T. Reid, "(87)Rb-stabilized 375-MHz Yb: fiber femtosecond frequency comb," *Opt. Express* **22**(9), 10494–10499 (2014).
14. G. Wang, F. Meng, C. Li, T. Jiang, A. Wang, Z. Fang, and Z. Zhang, "500 MHz spaced Yb: fiber laser frequency comb without amplifiers," *Opt. Lett.* **39**(9), 2534–2536 (2014).
15. D. Hou, J. Wu, S. Zhang, Q. Ren, Z. Zhang, and J. Zhao, "A stable frequency comb directly referenced to rubidium electromagnetically induced transparency and two-photon transitions," *Appl. Phys. Lett.* **104**(11), 111104 (2014).
16. Y. Kim, S. Kim, Y. J. Kim, H. Hussein, and S. W. Kim, "Er-doped fiber frequency comb with mHz relative linewidth," *Opt. Express* **17**(14), 11972–11977 (2009).
17. T. Kessler, C. Hagemann, C. Grebing, T. Legero, U. Sterr, F. Riehle, M. J. Martin, L. Chen, and J. Ye, "A sub-40-mHz-linewidth laser based on a silicon single-crystal optical cavity," *Nat. Photonics* **6**(10), 687–692 (2012).
18. D. Gatti, T. Sala, A. Gambetta, N. Coluccelli, G. N. Conti, G. Galzerano, P. Laporta, and M. Marangoni, "Analysis of the feed-forward method for the referencing of a CW laser to a frequency comb," *Opt. Express* **20**(22), 24880–24885 (2012).
19. Y. Zhang, L. Yan, S. Fan, L. Zhang, and W. Zhao, W. Guo, S. Zhang, and H. Jiang, "Development of an erbium-fiber-laser-based optical frequency comb at NTSC," *IFCS-EFTF, IEEE*, 599–601 (2015).
20. F. C. Cruz, G. Ycas, D. L. Maser, and S. A. Diddams, "Frequency stabilization of a mid-infrared optical frequency comb to single-frequency optical references," *MICS, OSA, MM1C*, 2 (2016).
21. N. Kuse, C. C. Lee, J. Jiang, C. Mohr, T. R. Schibli, and M. E. Fermann, "Ultra-low noise all polarization-maintaining Er fiber-based optical frequency combs facilitated with a graphene modulator," *Opt. Express* **23**(19), 24342–24350 (2015).
22. W. Hänsel, M. Giunta, K. Beha, M. Lezius, M. Fischer, and R. Holzwarth, "Ultra-low phase noise all-PM Er: fiber optical frequency comb," *ASSL, OSA, AT4A*, 2 (2015).
23. E. Baumann, F. R. Giorgetta, J. W. Nicholson, W. C. Swann, I. Coddington, and N. R. Newbury, "High-performance, vibration-immune, fiber-laser frequency comb," *Opt. Lett.* **34**(5), 638–640 (2009).
24. N. Daniele, B. Argence, W. Zhang, R. L. Targat, G. Santarelli, and Y. L. Coq, "Spectral Purity Transfer between Optical Wavelengths at the  $10^{-18}$  Level," *Nat. Photonics* **8**(3), 219–223 (2014).
25. M. Yan, W. Li, K. Yang, H. Zhou, X. Shen, Q. Zhou, Q. Ru, D. Bai, and H. Zeng, "High-power Yb-fiber comb with feed-forward control of nonlinear-polarization-rotation mode-locking and large-mode-area fiber amplification," *Opt. Lett.* **37**(9), 1511–1513 (2012).
26. C. C. Lee, C. Mohr, J. Bethge, S. Suzuki, M. E. Fermann, I. Hartl, and T. R. Schibli, "Frequency comb stabilization with bandwidth beyond the limit of gain lifetime by an intracavity graphene electro-optic modulator," *Opt. Lett.* **37**(15), 3084–3086 (2012).
27. J. A. Cox, A. H. Nejadmalayeri, J. Kim, and F. X. Kärtner, "Complete characterization of quantum-limited timing jitter in passively mode-locked fiber lasers," *Opt. Lett.* **35**(20), 3522–3524 (2010).
28. Y. Song, K. Jung, and J. Kim, "Impact of pulse dynamics on timing jitter in mode-locked fiber lasers," *Opt. Lett.* **36**(10), 1761–1763 (2011).
29. Y. Song, C. Kim, K. Jung, H. Kim, and J. Kim, "Timing jitter optimization of mode-locked Yb-fiber lasers toward the attosecond regime," *Opt. Express* **19**(15), 14518–14525 (2011).
30. P. Pal, W. H. Knox, I. Hartl, and M. E. Fermann, "Self referenced Yb-fiber-laser frequency comb using a dispersion micromanaged tapered holey fiber," *Opt. Express* **15**(19), 12161–12166 (2007).
31. C. Benko, A. Ruehl, M. J. Martin, K. S. E. Eikema, M. E. Fermann, I. Hartl, and J. Ye, "Full phase stabilization of a Yb: fiber femtosecond frequency comb via high-bandwidth transducers," *Opt. Lett.* **37**(12), 2196–2198 (2012).
32. T. R. Schibli, I. Hartl, D. C. Yost, M. J. Martin, A. Marcinkevicius, M. E. Fermann, and J. Ye, "Optical frequency comb with submillihertz linewidth and more than 10 W average power," *Nat. Photonics* **2**(6), 355–359 (2008).
33. A. Cingöz, D. C. Yost, T. K. Allison, A. Ruehl, M. E. Fermann, I. Hartl, and J. Ye, "Broadband phase noise suppression in a Yb-fiber frequency comb," *Opt. Lett.* **36**(5), 743–745 (2011).
34. L. Nugent-Glandorf, T. A. Johnson, Y. Kobayashi, and S. A. Diddams, "Impact of dispersion on amplitude and frequency noise in a Yb-fiber laser comb," *Opt. Lett.* **36**(9), 1578–1580 (2011).
35. D. Hou, B. Ning, S. Zhang, J. Wu, and J. Zhao, "Long-term stabilization of fiber laser using phase-locking technique with ultra-low phase noise and phase drift," *IEEE J. Sel. Top. Quantum Electron.* **20**(5), 456–463 (2014).
36. Y. Nakajima, H. Inaba, K. Hosaka, K. Minoshima, A. Onae, M. Yasuda, T. Kohno, S. Kawato, T. Kobayashi, T. Katsuyama, and F. L. Hong, "A multi-branch, fiber-based frequency comb with millihertz-level relative linewidths using an intra-cavity electro-optic modulator," *Opt. Express* **18**(2), 1667–1676 (2010).
37. F. Quinlan, T. M. Fortier, M. S. Kirchner, J. A. Taylor, M. J. Thorpe, N. Lemke, A. D. Ludlow, Y. Jiang, and S. A. Diddams, "Ultralow phase noise microwave generation with an Er: fiber-based optical frequency divider," *Opt. Lett.* **36**(16), 3260–3262 (2011).
38. S. Rieger, T. Hellwig, T. Walbaum, and C. Fallnich, "Optical repetition rate stabilization of a mode-locked all-fiber laser," *Opt. Express* **21**(4), 4889–4895 (2013).
39. B. J. Bloom, T. L. Nicholson, J. R. Williams, S. L. Campbell, M. Bishof, X. Zhang, W. Zhang, S. L. Bromley, and J. Ye, "An optical lattice clock with accuracy and stability at the  $10^{-18}$  level," *Nature* **506**(7486), 71–75 (2014).
40. L. Hou, H. Han, L. Zhang, J. Zhang, D. Li, and Z. Wei, "A narrow linewidth diode laser at 243 nm," *Wuli Xuebao* **64**(13), 134205 (2015).

41. R. J. Rafac, B. C. Young, J. A. Beall, W. M. Itano, D. J. Wineland, and J. C. Bergquist, "Sub-dekahertz ultraviolet spectroscopy of  $199\text{Hg}^+$ ," *Phys. Rev. Lett.* **85**(12), 2462–2465 (2000).
42. K. Iwakuni, H. Inaba, Y. Nakajima, T. Kobayashi, K. Hosaka, A. Onae, and F. L. Hong, "Narrow linewidth comb realized with a mode-locked fiber laser using an intra-cavity waveguide electro-optic modulator for high-speed control," *Opt. Express* **20**(13), 13769–13776 (2012).
43. M. Hoffmann, S. Schilt, and T. Südmeyer, "CEO stabilization of a femtosecond laser using a SESAM as fast opto-optical modulator," *Opt. Express* **21**(24), 30054–30064 (2013).
44. D. W. Allan, "Time and frequency (time-domain) characterization, estimation, and prediction of precision clocks and oscillators," *IEEE Trans. Ultrason. Ferroelectr. Freq. Control* **34**(6), 647–654 (1987).
45. P. Lesage, "Characterization of frequency stability: bias due to the juxtaposition of time-interval measurements," *IEEE Trans. Instrum. Meas.* **32**(1), 204–207 (1983).
46. I. Ushijima, M. Takamoto, M. Das, T. Ohkubo, and H. Katori, "Cryogenic optical lattice clocks," *Nat. Photonics* **5**, 203–210 (2015).
47. T. L. Nicholson, S. L. Campbell, R. B. Hutson, G. E. Marti, B. J. Bloom, R. L. McNally, W. Zhang, M. D. Barrett, M. S. Safronova, G. F. Strouse, W. L. Tew, and J. Ye, "Systematic evaluation of an atomic clock at  $2 \times 10^{-18}$  total uncertainty," *Nat. Commun.* **6**, 6896 (2015).

## 1. Introduction

The development of modern science and technology depends on precision optical interferometers. Optical frequency comb (OFC) pushes the measurement of optical frequencies to extreme [1–3], acting as precision and coherent link between optical and microwave frequencies. The simple operation, reliability and versatility of OFC have turned it into a powerful tool that opens new frontiers in such fields as terahertz technology, astro-comb, distance measurement, molecule spectroscopy, low noise microwave generation, optical clocks, time and frequency transfer [4–11]. Oftentimes among those application fields, the frequency stability and phase noise are extremely important parameters. Thus, achieving a reliable phase-locking technique with ultra-low phase noise and ultra-stability is a key issue in the design of long-term stabilization systems.

OFC can be expressed as  $f_n = f_{ceo} + n + f_r$ , where  $f_{ceo}$  is the carrier envelope offset (CEO) frequency, responsible for the drift removing of the entire optical comb modes. The  $f_r$  is the repetition rate,  $n$  is an integer of  $10^5 - 10^6$ , so a small frequency fluctuation of  $f_r$  can lead to a significant frequency variation of  $f_n$ . Consequently,  $f_r$  definitely needs controlling in a high bandwidth to overcome the unexpected changes introduced by environmental noises or others. The stability of  $f_{ceo}$  and  $f_r$  determines the frequency accuracy of each comb tooth  $f_n$ . The accuracy of the reference source determines the frequency stability of the  $f_{ceo}$  and  $f_r$ . Limited to the stability of Rb microwave clock of about  $10^{-12}/\text{s}$ , the frequency stability has reached  $10^{-13}/\text{s}$  as the superior results [12–16]. Ye et al. has used the silicon single-crystal optical cavity to reduce the thermal noise, get the fractional frequency instability of  $10^{-16}$  at  $1.5 \mu\text{m}$  [17]. Refer to optical frequency standard such as CW laser; the relative frequency stability of  $f_r$  is  $\sim 2.1 \times 10^{-16}/\text{s}$  in Er-doped fiber OFC [18–21]. Locked to the cavity-stabilized CW laser, the  $f_r$  exhibits an Allan variance below  $10^{-16}/\text{s}$  in all-PM Er-doped fiber OFC [22, 23]. In Ref [24], an optical frequency comb-based scheme that transfers from a 1062 nm laser to a 1542 nm laser, and the  $4.5 \times 10^{-16}$  fractional frequency stability is down to  $4 \times 10^{-18}$  at 1 s with cavity-stabilized 1542 nm laser as reference source.

Fiber-based OFC based on nonlinear polarization rotation (NPR) [25] or saturable absorber (SA)-assisted NPR mode-locking mechanisms have proven to be viable alternatives, and have also been operated at low values of phase noise [26–29]. Owing to the operation wavelength covering telecom band, Er-doped fiber OFC becomes mature and commercial. As the high efficiency, high power and broad spectral coverage, Yb-doped fiber laser have been a good choice for OFCs [12, 14, 30–34].

In this paper, we lock the Yb-doped fiber OFC to an ultra-stable CW laser. The ultra-stable CW laser is realized by locking a hyperfine Fabry-Perot (FP) cavity to the 972 nm CW laser with the Pound-Drever-Hall (PDH) technique. The Yb-doped fiber OFC source is 250 MHz

Yb-doped fiber mode-locked oscillator based on the NPR mechanism (Menlosystems GmbH). By using the standard PLL technique, the  $f_{ceo}$  with SNR of 40 dB under 300 kHz RBW is stabilized to the RF synthesizer, the standard deviation from 20 MHz reference frequency 6.26 mHz over 13 hours, the Allan variance reaches  $1.2 \times 10^{-17}/s$ , averaging down below  $8.3 \times 10^{-19}/100s$ . The  $f_r$  is controlled by locking the beat signal between Yb-doped fiber OFC and CW laser. Two stage fiber amplifier, compressor and broaden spectrum in photonic crystal fiber (PCF) are designed to enhance 972 nm components. The SNR of the  $f_{beat}$  signal is 43 dB at RBW of 300 kHz. The standard deviation is calculated to be 575  $\mu$ Hz over 3 hours, while the Allan variance reaches  $2 \times 10^{-18}/s$ . The integrate noise of phase (IPN) is 539 mrad from 1 Hz to 10 MHz, the corresponding time jitter is 278 as. To our knowledge, results are the highest frequency stability among Yb-doped fiber OFC. In addition, the linewidth was measured to subherz under the instrument-limited resolution bandwidth of 1 Hz, while the noise is suppressed over 40 dB.

## 2. Experimental results and discussion

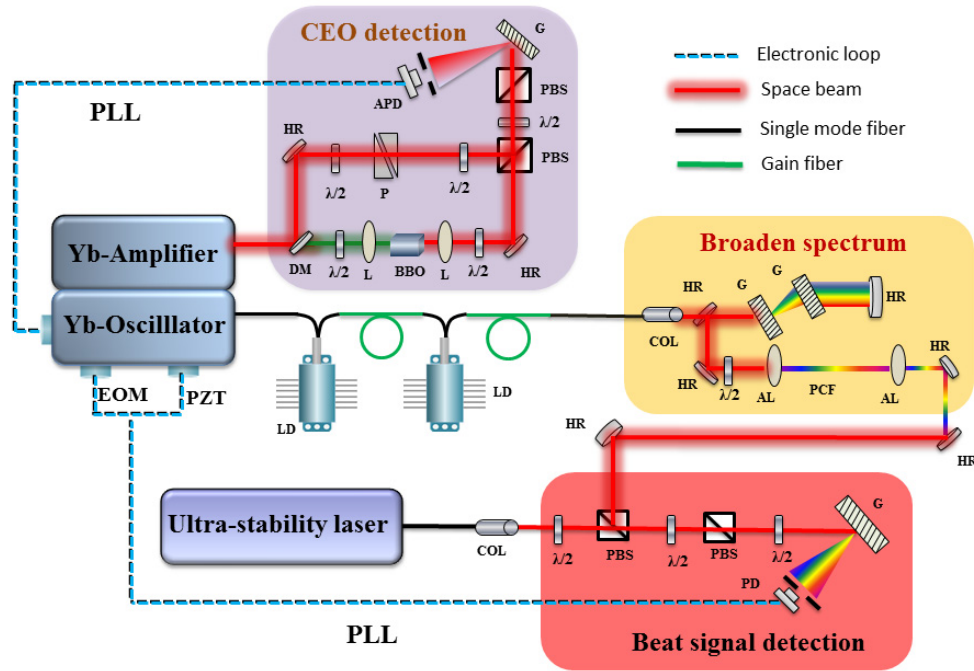


Fig. 1. Layout of the Yb-doped fiber OFC and feedback loop. EOM: electro optical modulator; PZT: piezoelectric transducer; PC: pump current; DM: dichroic mirrors; L: lenses;  $\lambda/2$ : half-wavelength plate; HR: high reflection mirror; P: prism pair; PBS: polarization beam splitter; G: grating; APD: avalanche photo diode; PLL: phase locked loop; Col: collimator; AL: aspherical lens; PCF: photonic crystal fiber; PD: photo diode.

### 2.1 Yb-doped fiber OFC

The Yb-doped fiber OFC includes four parts: Yb-doped fiber mode-locked oscillator, Yb-fiber amplifier, CEO detection system and PLL circuit [34], as schematically showed in Fig. 1. The oscillator based on the NPR mechanism is designed to provide chirped-pulses of 6.7 ps duration at 250 MHz repetition rate. The 3-dB optical spectrum width is about 40 nm, along with the center wavelength of 1040 nm. Especially, in the ring cavity, the PZT and EOM are added as feedback terminals to fine tune the  $f_r$  signal [35,36]. The Yb-doped amplifier module encapsulated is set to generate the supercontinuum.



We adopted the standard f-2f interference technique for the  $f_{ceo}$  signal detection. The  $f_{ceo}$  signal has a SNR of 40 dB at RBW of 300 kHz, as shown in Fig. 2(a), then the  $f_{ceo}$  signal is stabilized to the RF synthesizer with a standard PLL technique. By regulating the pump current and the insertion of intra-cavity wedge, the  $f_{ceo}$  signal is located in 20 MHz reference frequency [37]. We investigated the long-term stability of the locked  $f_{ceo}$  signal. The frequency offset from a 20 MHz reference frequency was recorded for more than 12 hours recorded by the counter at 1-s gate time and the standard deviation is calculated to be 6.25 mHz, as shown in Fig. 2(b). The Allan variance to the optical laser frequency ( $\lambda_{opt} = 1040$  nm) is  $1.2 \times 10^{-17}$  at 1s-gate time and averaging down below  $8.3 \times 10^{-19}$  at 100 s, as shown in Fig. 2(c). Such stability is good enough to be compared with optical atomic clocks with frequency stability of  $\sim 3.2 \times 10^{-16}$  [38].

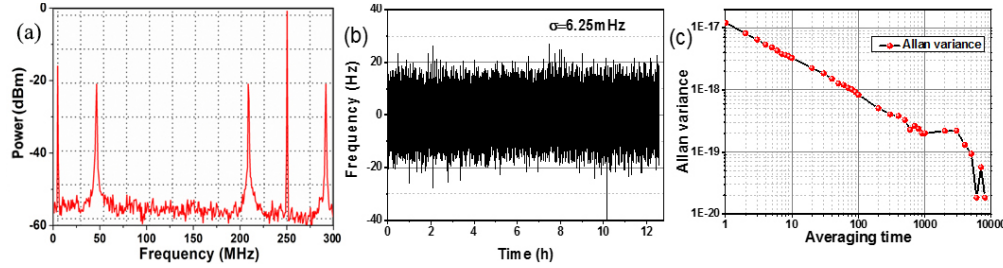


Fig. 2. (a) The  $f_{ceo}$  signal with SNR of 40 dB at the RBW = 300 kHz; (b) The frequency deviation of the locked  $f_{ceo}$  signal for about 13 hours recorded by the counter at 1s gate time; (c) The corresponding Allan deviation to the optical laser frequency  $\nu_{opt}$  ( $\lambda_{opt} = 1040$  nm).

## 2.2 The broadened spectrum

In our laboratory, there is an established ultra-stable narrow linewidth 972 nm CW laser to detect hydrogen atoms 1S-2S energy level transition spectrum line [39]. The 972 nm ultra-stability FP cavity using the PDH technique, and the cavity finesse is measured to be 208600, corresponding to the cavity linewidth of 7.2 kHz, which can fully meet requirement that the ultra-stable laser linewidth is narrowed to Hz and even subhertz magnitude. The CW laser with subhertz linewidth is essential to push the frequency uncertainties with optical atomic frequency standards toward the  $10^{-18}$  level [40].

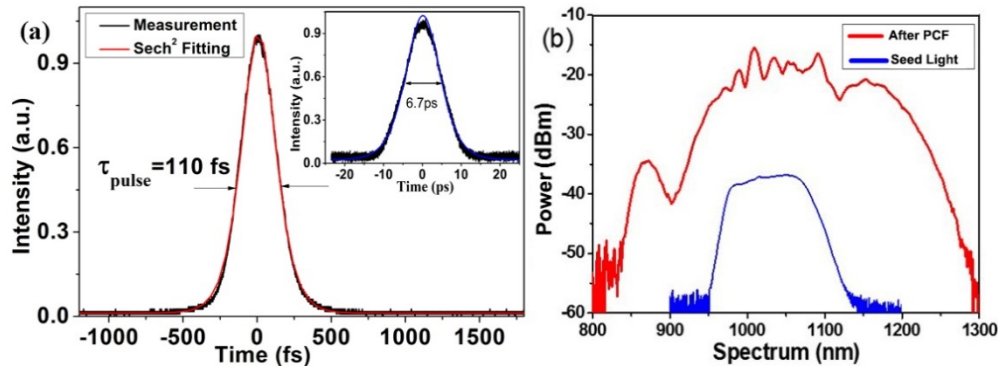


Fig. 3. (a) The pulse width of 110 fs compressed from 6.7 ps seed light; (b) The broadened spectrum covering 972 nm component, the red line is the amplification light and the blue line is seed light.

The  $f_r$  is set to be locked to the ultra-stability narrow linewidth CW laser. Due to the 972 nm component directly from the Yb-doped fiber OFC is too weak to generate beat signal, the

seed light with 18 mW from Yb-fiber oscillator was delivered to two stage Yb-doped fiber amplify: preamplifier pump power is 500 mW and the main amplifier is 4 W. Due to the existence of negative chirp in the seed laser, there is no nonlinear mechanism in the amplification process, the amplitude-to-phase noise is eliminated effectively [31]; then the amplified laser is compressed by a pair of projection grating. The schematic diagram is shown in Fig. 1. The terminal output is 110 fs pulse width close to Fourier-transform limit, and 1.6 W average output power, as shown in Fig. 3(a), was coupled into PCF (SC-5.0-1040, NKT) to broaden spectrum covering 972 nm component, as shown in Fig. 3(b).

### 2.3 The beat signal detection and stability

The broadened spectrum from the PCF is heterodyned against the narrow linewidth 972 nm CW laser to produce a  $f_{beat}$  signal. We compared the performance of three photodetectors in our lab, such as C5658APD (Hamamatsu, center wavelength@800 nm), EOT2040 (Electro-Optics Technology, Inc., center wavelength@950 nm) and home-made PD (wavelength@800 nm). The home-made PD is found with the highest signal-to-noise ratio for beat signal. Amazing that the SNR of  $f_{beat}$  reaches to 43 dB at 300 kHz RBW, according to Fig. 4 (a), which is higher than the typical value of 30 dB for common feedback circuit. The peak intensity is about -67 dBm much less than -40 dBm (the minimum power requirement of circuit). We designed two stage circuit amplifiers to improve the peak intensity from -67 dBm to -20 dBm. The EOM and PZT act as fast loop and slow loop respectively to lock the optical frequency  $f_{beat}$ . The PZT with a few kHz servo bandwidth alone cannot reduce the residual phase noise, EOM with a broad servo bandwidth of about 1 MHz to narrow the  $f_{beat}$  linewidth [41]. By double loop lock, the 200 kHz (RBW = 1 kHz) linewidth is narrowed to subhertz under the instrument-limited resolution bandwidth of 1 Hz by a spectrum analyzer (R&S, FSW26), 10 Hz range near peak spectrum as shown in Fig. 4(b), indicating the lock system has an excellent suppression to the noise of  $f_{beat}$ . Under RBW of 10 Hz, we obtained a in-loop beat spectra (RBW = 10 Hz) in Fig. 4(c), and the serve bandwidth is about 350 kHz in loop. More than 40 dB suppression is achieved, showing that in-loop beat signal concentrates 90% up energy of the RF power. The actual bandwidth of the whole feedback system is about 350 kHz under RBW of 10 Hz, less than servo bandwidth of 1 MHz, limited by the upper lifetime of the Yb-doped laser [42]. Then we measured the IPN of the beat signal. As shown in Fig. 4(d), the IPN is about 539 mrad, integrated from 1 Hz to 10 MHz, the noise between 1 Hz to 350 kHz is obviously suppressed, and the corresponding time jitter is 278 as, indicating excellent control over the frequency comb mode.

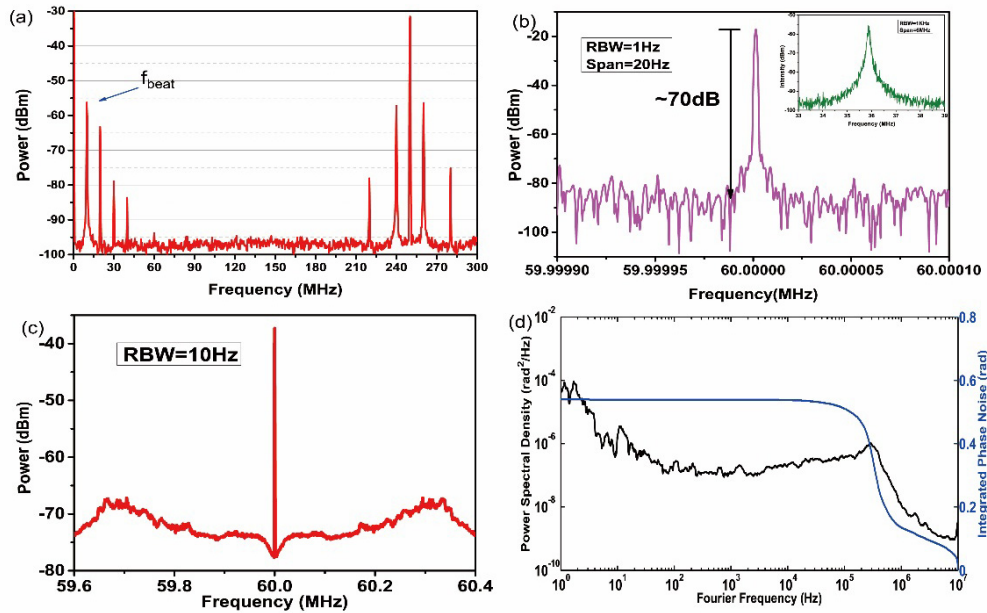


Fig. 4. (a) The  $f_{beat}$  signal with SNR of 43 dB at the RBW = 300 kHz; (b) Out of lock, the linewidth of the beat signal is about 200 kHz at RBW = 1 kHz; (c) In loop, the RF spectrum of beat observed with a spectrum analyzer. The spectrum is clean and its energy concentration to the coherent carrier is more than 90% at a bandwidth of 10 Hz; (d) The IPN is about 539 mrad from 1 Hz to 10 MHz.

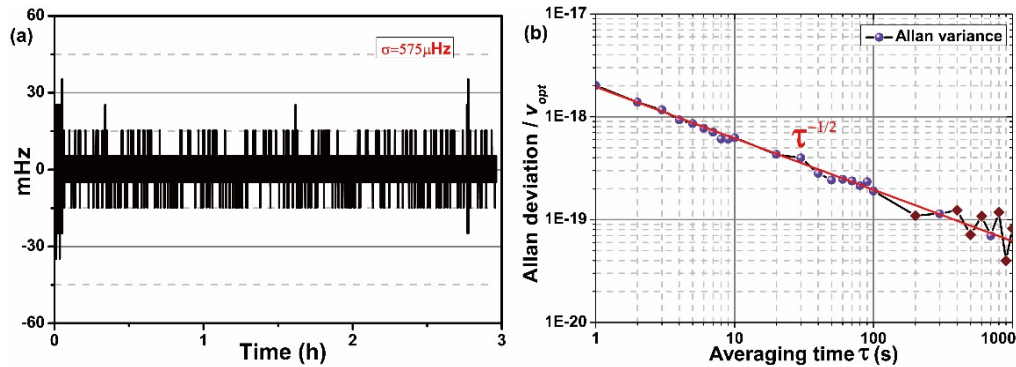


Fig. 5. (a) The frequency deviation of the locked  $f_{beat}$  signal for about 13 hours recorded by the counter at 1-s gate time; (b) The corresponding Allan deviation to the optical laser frequency  $\nu_{opt}$  ( $\lambda_{opt} = 972 \text{ nm}$ ).

Furthermore, we investigated the long-term stability of the locked beat signal. The locked  $f_{beat}$  signal was counted with a universal counter in 1 s of gate time. The frequency offset from a 60 MHz reference was recorded for almost 3 hours using an rf frequency counter (53131A, Agilent), and the gate time is 1s, and the standard deviation is calculated to be 575  $\mu\text{Hz}$ , according to Fig. 5(a). The 575  $\mu\text{Hz}$  standard deviation shows higher tracking stability for PLL system. The 43 dB high SNR (RBW = 300 kHz) of beat signal and commercial technologies such as vibration isolation and temperature control on laser oscillator provide guarantees for precision lock. The IPN is 539 mrad (or the time jitter of 278 as) integrated from 1 Hz to 10 MHz, especially the low frequency noise (about 0.022 mrad under 350 kHz) mainly induced by environmental perturbation is effectively suppressed. These indicate that the standard deviation of 575  $\mu\text{Hz}$  is in high precision locking state.

The calculated corresponding Allan deviation in a juxtaposed manner is shown in Fig. 5(b), which shows a tracking stability of  $2.0 \times 10^{-18}/\text{s}$  at the central wavelength of 972 nm, averaging down below  $8.1 \times 10^{-20}$  at 1000 s gate time. The slope is proportional to  $\tau^{-1/2}$ , where  $\tau$  is the gate time. The characteristics of the white frequency noise are presented through the agreement of the standard deviation and the Allan deviation at 1s. It can also be confirmed by the  $\tau^{-1/2}$  dependence of the Allan deviation [44]. For the white frequency noise, the Allan variance calculation will be resulted by the juxtaposed measurement [45]. The  $2 \times 10^{-18}/\text{s}$  frequency stability with 1s gate time is only  $2.0 \times 10^{-18}$  and the ultralow residual phase noise while phase-locked by far surpass the stability of today's best atomic clocks [46, 47].

### 3. Conclusion

We have reported a full control ultra-stability Yb-doped fiber OFC. The CEO has been stabilized to the RF synthesizer by controlling the pump current and the insertion of intracavity wedge. The standard deviation has been calculated to be 6.25 mHz in almost 13 hours. The Allan variance is  $1.2 \times 10^{-17}$  at 1s-gate time and averaging down below  $8.3 \times 10^{-19}$  at 100 s. For heterodyne between Yb-doped fiber OFC and 972 nm CW laser, two stage fiber amplifier, grating compressor and the PCF have been involved to improve the 972 nm component intensity. The  $f_{\text{beat}}$  signal has been attained with SNR of 43 dB (at 300 kHz RBW) with common heterodyne technique. We have locked the beat signal with PZT and EOM act as the slow loop and fast loop, the linewidth of the beat signal has been narrowed from 200 kHz out of loop to subhertz magnitude in instrument-limited resolution bandwidth. The IPN has been measured with 539 mrad, the corresponding time jitter has been about 278 as. The standard deviation has been calculated to be 575  $\mu\text{Hz}$  in almost 3 hours, and the Allan deviation has been only  $2.0 \times 10^{-18}/\text{s}$ , and  $8.1 \times 10^{-20}$  in 1000-s gate time at the central wavelength of 972 nm, which corresponds to the high stability among Yb-doped fiber based OFC.

### Funding

We thank the funding supports by the National Basic Research Program of China (973 Program Grant No. 2012CB821304), and the National Natural Sciences Foundation of China (Grant Nos. 11674036, 11078022 and 61378040).